Erin A. S. Doherty[1]
K. Derek Berglund[2]
Brett A. Buchholz[1]
Igor V. Kourkine[1]
Todd M. Przybycien[2]
Robert D. Tilton[2]
Annelise E. Barron[1]

[1]Department of Chemical Engineering, Northwestern University, Evanston, IL, USA
[2]Department of Chemical Engineering and the Center for Complex Fluids Engineering, Carnegie Mellon University, Pittsburgh, PA, USA

Critical factors for high-performance physically adsorbed (dynamic) polymeric wall coatings for capillary electrophoresis of DNA

Physically adsorbed (dynamic) polymeric wall coatings for microchannel electrophoresis have distinct advantages over covalently linked coatings. In order to determine the critical factors that control the formation of dynamic wall coatings, we have created a set of model polymers and copolymers based on *N,N*-dimethylacrylamide (DMA) and *N,N*-diethylacrylamide (DEA), and studied their adsorption behavior from aqueous solution as well as their performance for microchannel electrophoresis of DNA. This study is revealing in terms of the polymer properties that help create an "ideal" wall coating. Our measurements indicate that the chemical nature of the coating polymer strongly impacts its electroosmotic flow (EOF) suppression capabilities. Additionally, we find that a critical polymer chain length is required for polymers of this type to perform effectively as microchannel wall coatings. The effective mobilities of double-stranded (dsDNA) fragments within dynamically coated capillaries were determined in order to correlate polymer hydrophobicity with separation performance. Even for dsDNA, which is not expected to be a strongly adsorbing analyte, wall coating hydrophobicity has a deleterious influence on separation performance.

Keywords: DNA separation / Microchannel electrophoresis / Polymeric wall coating EL 4942

1 Introduction

Rapid, efficient biomolecule separations within glass capillaries and microfluidic devices will be critical in the post-genome era, in which diagnostic applications, including genetic mutation detection and protein and peptide separation and quantitation by electrophoresis, will play an expanding role [1]. In order to obtain high-efficiency, reproducible biomolecule separations in fused-silica or glass microchannels, a wall coating is required to reduce or eliminate analyte-wall interactions and to suppress electroosmotic flow (EOF) [2, 3]. Coating the microchannel wall with a polymer layer shifts the hydrodynamic plane of shear away from the underlying charged surface, and hence minimizes or nearly eliminates EOF since EOF is directly related to the magnitude of the zeta potential [4–7]. Ideally, for DNA separations, which are the primary focus of our research, a wall coating would be charge-neutral, hydrolytically stable, at least as thick as the electrical double layer, and simple to form at the wall.

Correspondence: Professor Annelise E. Barron, Northwestern University, Department of Chemical Engineering, 2145 Sheridan Road, Room E136, Evanston, IL 60208, USA
E-mail: a-barron@northwestern.edu
Fax: +847-491-3728

Abbreviations: **DEA**, *N,N*-diethylacrylamide; **DMA**, *N,N*-dimethylacrylamide; **LPA**, linear polyacrylamide; **PDEA**, poly(*N,N*-diethylacrylamide); **PDI**, polydispersity index; **PDMA**, poly(*N,N*-dimethylacrylamide)

Many different synthetic polymeric wall coatings have been developed in order to improve the separation efficiency and the reproducibility of biomolecule separations [3, 8]. One of the most widely used wall coatings for EOF suppression in microchannel electrophoresis was introduced in 1985 by Hjertén [5]. This coating, based on *in situ* polymerized linear polyacrylamide (LPA), consists of a layer of uncharged, hydrophilic polymeric material covalently cross-linked to the lumen of the capillary. Covalently bound LPA coatings work well while fresh, suppressing EOF and minimizing biomolecule interaction with the microchannel wall. However, LPA coatings have limited stability and lifetime. To address these limitations, other covalently bound coatings have been developed, including those based on poly(vinyl alcohol) (PVA) [9, 10], poly(acryloylaminoethoxy-ethanol) (poly(AAEE)) [11], and others [12–17]. Some covalently linked coatings, including PVA and poly(AAEE), can be stable for over 100 runs [10].

The production of covalently linked LPA, like the production of many other covalently linked polymeric coatings, is time-consuming and generates an uneven layer of material of unknown thickness [17]. In addition, the reproducible formation of covalently linked coatings is highly dependent on initial glass surface chemistry. For these reasons, *in situ* polymerized coatings can be difficult to control, optimize and quality control. Moreover, LPA coatings hydrolyze fairly rapidly under the high pH, aqueous conditions of DNA electrophoresis, leading to a ten-fold

 0173-0835/02/1608–2766 $17.50+.50/0

increase in the electroosmotic mobility (μ_{EOF}) over 80 h [11]. Finally, the *in situ* polymerization step necessary to create covalently linked coatings, which results in the formation of a viscous polymer solution in the capillary lumen that must be expelled under high pressure, limits their practicality for use in small-inner diameter microchannels [2].

The adverse effects of variable glass surface chemistry on wall coating formation can be minimized through the use of so-called "dynamic" or adsorptive coatings. Although numerous methods of dynamic EOF suppression exist, most dynamic coatings for DNA sequencing are produced by microchannel flushing with low-viscosity aqueous solutions of an adsorbing polymer, which obviates the need for organic solvents, high temperatures, and viscous solutions, all of which are required to produce covalently linked coatings [18]. Dynamic coatings have additional advantages over covalently linked coatings, including the possibility for coating automation and coating regeneration and access to *a priori* knowledge of polymer physical properties, facilitating quality control. Although the mechanism of formation of adsorbed polymer coatings has not been carefully investigated by CE researchers, these physically adsorbed coatings are thought to form at the silica surface because of either hydrophobic [2], electrostatic [19–21], or hydrogen bonding [22] interactions of the coating material with the walls, neither of which rely as strongly on the density of reactive alcohol groups on the wall surface as silanization.

Polymers that have been investigated as adsorptive polymeric wall coatings for microchannel electrophoresis include poly(*N,N*-dimethylacrylamide) (PDMA) [23], polyvinylpyrrolidone (PVP) [24], and a variety of other novel, acrylamide-based polymers [2, 25–27]. At this time, PDMA and PVP are the most widely used adsorptive wall coatings for biomolecule analysis. The most significant disadvantage of most presently available dynamic coatings is their reduced effectiveness for protein separations due to polymer hydrophobicity, which is thought to increase analyte-wall interactions [3, 28]. Therefore, it is desirable to minimize polymer hydrophobicity, while still retaining dynamic coating ability. A better understanding of the relationship between polymer properties and coating performance could allow for rational design of an optimized, polymeric wall coating for protein separations.

In this work, we correlate the chemical and physical nature of *N,N*-disubstituted acrylamide polymers with their ability to provide an adsorptive wall coating useful for biomolecule separations. Adsorption behavior of dynamic wall coatings based on polymers of PDMA, poly(*N,N*-diethylacrylamide) (PDEA), and *N,N*-diethylacrylamide/*N,N*-dimethylacrylamide (DEA/DMA) random copolymers was studied by scanning angle reflectometry and streaming current measurements. Coating performance was also quantitatively analyzed *in situ* by measuring the electroosmotic mobility (μ_{EOF}) within a coated microchannel, and by separating a model analyte, dsDNA, within dynamically coated microchannels filled with a low-molar-mass LPA separation matrix. The effect of polymer contour length on EOF suppression was investigated as well, in order to determine a possible threshold contour length for the acceptable suppression of EOF. This study indicates that control of both polymer contour length and hydrophilicity are critical requirements for the successful use of dynamic wall coatings for CE separations.

2 Materials and methods

2.1 Reagents

Tris, ethylenediaminetetraacetic acid (EDTA), ultrapure-grade *N,N,N',N'*-tetraethylmethylenediamine (TEMED) and ammonium persulfate (APS) were purchased from Amresco (Solon, OH, USA). *N*-[Tris(hydroxymethyl)-methyl]-3-aminopropanesulfonic acid (TAPS), morpholinoethanesulfonic acid (MES), and lithium hydroxide monohydrate were obtained from Sigma (St. Louis, MO, USA). Benzyl alcohol (99+%) was purchased from Aldrich (Milwaukee, WI, USA). Deuterated water (100% D) and deuterated chloroform (99.8% D) were purchased from Acros (Pittsburgh, PA, USA). Ultrapure DMA (99.5%) and DEA (99.5%) were purchased from Monomer-Polymer and Dajac Laboratories (Feasterville, PA, USA). Hydroquinone/methyl ester remover packing was purchased from Scientific Polymer Products, (Ontario, NY, USA). Azo-type bis-initiator V-50 (2,2'-azobis(2-amidinopropane) dihydrochloride) was purchased from Wako Pure Chemical Industries (Osaka, Japan). DNA digest pBR322-*Msp*I was purchased from New England BioLabs (Beverly, MA, USA). Nitrocellulose membranes (pore size 0.025 μm) were from Millipore (Bedford, MA, USA). Chromerge® cleaning solution, ACS-grade hydrochloric acid, and ACS-grade sulfuric acid were purchased from Fisher Scientific (Pittsburgh, PA, USA); ACS-grade sodium hydroxide was from EM Science (Gibbstown, NJ, USA). Chromerge® was prepared by mixing 25 mL of the Chromerge® cleaning solution with 2.5 L of 2.5 N sulfuric acid. All solutions for scanning angle reflectometry measurements were contained in Chromerge®-cleaned glassware. Water used for scanning angle reflectometry and streaming current measurements was purified by reverse osmosis followed by treatment by Milli-Q Plus ion exchange and organic adsorption cartridges (Millipore).

2.2 Polymer synthesis

PDMA, PDEA, DEA/DMA copolymers, and LPA that were matched for contour length were polymerized in an aqueous solution (7.0 w/w% total monomer concentration) thermostatted at 47°C and deoxygenated with high purity helium prior to initiation. V-50 initiator was dissolved in water and injected into the reaction flask through a rubber septum. After 16 h, the resulting polymer solution was allowed to come to room temperature. LPA employed as the DNA separation matrix as well as PDMA and LPA having weight average molar masses under 2.0 MDa were polymerized in aqueous solution (9.1 w/w% total monomer concentration) thermostatted at 50°C and deoxygenated with nitrogen prior to initiation by 10% APS and TEMED in equal volume. Molar mass was controlled using isopropanol as a chain transfer agent; polymerization was stopped using an ice bath after 1.5 h. Resulting reaction mixtures were immediately poured into 1000 Da molecular weight cutoff (MWCO) cellulose ester membranes (Fisher Scientific), and dialyzed against deionized, distilled water for 10 days with frequent water changes. The polymer solution was then frozen and lyophilized using a freeze-dry system (Labconco, Kansas City, MO, USA), resulting in a white, stiff, foam-like mass that was then redissolved in aqueous buffer by slow rotation for 24 h (Roto-Torque, Cole-Parmer Instrument Company, Vernon Hills, IL, USA).

2.3 Polymer characterization

To characterize the molar mass distributions of the polymers and copolymers that were synthesized, samples were fractionated by gel permeation chromatography (GPC) prior to analysis by on-line multiangle laser light scattering (MALLS) and refractive index detection, as described previously [29]. ^{1}H NMR was performed with a Varian INOVA 500 (Walnut Creek, CA, USA) to determine the composition of the DMA/DEA copolymers and the actual proportions of each monomer incorporated into the copolymers, as previously described [29].

2.4 Capillary coating

A series of fused-silica capillaries (Polymicro Technologies, Phoenix, AZ, USA) with a nominal ID of 50 μm were dynamically coated with LPA, PDMA, PDEA, and DEA/DMA random, linear copolymers in order to compare their tendencies to form adsorbed capillary coatings. Our protocol was implemented using a Beckman P/ACE 5000 Series Capillary Electrophoresis System (Fullerton, CA, USA). Pretreatment of the capillary included the following: 15 min flush with 1 M NaOH at 20 psi (all pressures were applied with positive nitrogen flow), 15 min flush with 0.1 M NaOH at 20 psi, and 15 min flush with water at 20 psi. Capillary coating was accomplished using a 20 min flush with a 0.1 w/v% solution of polymer in water at 20 psi, followed by a 5 min flush with water at 20 psi, and a 5 min flush with background electrolyte (BGE) buffer (30 mM morpholinoethanesulfonic acid, 67 mM lithium hydroxide monohydrate) at 20 psi.

2.5 EOF measurement

The electroosmotic mobility was measured immediately prior to and following the dynamic coating procedure using the protocol developed by Williams *et al.* [30] and the Beckman P/ACE 5000. Briefly, three peaks of a neutral marker, benzyl alcohol, are used to quantitatively determine the electroosmotic mobility. First, the capillary is filled with BGE buffer. Then, two bands of neutral marker, separated by BGE buffer, are pushed into the capillary under positive nitrogen pressure a specified distance apart. An electric field is applied, under which the two neutral peaks will migrate due to EOF. After the electric field is removed, a third neutral band is injected under nitrogen pressure and all three peaks are pushed past the detector by filling the capillary with BGE buffer under nitrogen pressure. The distance between the second and third peaks is then measured, and may be related to the electroosmotic mobility. Peak migration times were determined using Beckman P/ACE Station Version 1.1 Software.

2.6 Scanning angle reflectometry

Reflectometry experiments were performed on optical-grade silicon wafers purchased from Valley Design Corporation (Westford, MA, USA) and thermally oxidized to produce silicon oxide surface layers. The substrate was cleaned with Chromerge® and then with 6.0 M hydrochloric acid prior to being stored in water. Prior to experiments, the substrate was rinsed profusely with water and then treated with base in the same manner as the silica capillaries to start the experiment. Once cleaned, the wafers were never allowed to dry. Adsorbed polymer surface excess concentrations were measured using optical reflectometry. Principles and applications of optical reflectometry are described elsewhere, as are detailed descriptions of the particular instrument used in our experiments [31–33]. Polymers were adsorbed to the flat silica surfaces at 25°C from unbuffered, 0.1 w/v% aqueous solutions undergoing steady laminar slit flow at a wall shear rate of 1.0 s^{-1}. Each solution made a single pass over the surface without recycling to avoid the introduction of impurities. Conversion from raw reflectivity data to surface excess concentrations was based on a

two-layer striated interface optical model (oxide layer + adsorbed layer), using the polymer refractive index increments, d*n*/d*c*, which were measured independently.

2.7 Streaming current measurements

Since optical reflectometry does not directly provide the thickness of the adsorbed polymer layer, the layer thicknesses were determined *via* streaming current measurements. Thicknesses measured are referred to as "electrokinetic layer thicknesses", which closely match hydrodynamic layer thicknesses [6]. Streaming current measurements were made on soda lime glass slides (Fisher Scientific) that were first treated with sulfuric acid to provide surface chemistry that is very similar to pure silica [34]. The substrate was then cleaned and stored in the same manner as the substrates used in the scanning angle reflectometry experiments. For the neutral polymers considered here, the electrokinetic layer thickness is determined by measuring the zeta potential before and after adsorption ([6, 35]; Braem *et al.*, in preparation). By shifting the plane of shear further from the solid surface, the adsorbed layer decreases the magnitude of the zeta potential relative to the bare surface potential. Assuming the polymer layer does not perturb the electrostatic double layer, the polymer layer thickness, *d*, may be calculated from the measured zeta potentials before, ζ_o, and after, ζ_{ads}, adsorption, according to Gouy-Chapman theory:

$$\zeta_{ads} = \frac{2kT}{e}\ln\left[\frac{1+\tanh\left(\frac{e\zeta_0}{4kT}\right)\exp(-\kappa d)}{1-\tanh\left(\frac{e\zeta_0}{4kT}\right)\exp(-\kappa d)}\right] \quad (1)$$

where κ is the inverse Debye length, *e* is the elemental charge, *T* is the temperature, and *k* is Boltzmann's constant. Instrumental and theoretical issues, particularly concerning the advantage of streaming current measurements over streaming potential measurements, are described elsewhere ([35]; Braem *et al.*, in preparation). Zeta potentials of the bare surfaces were measured in 0.1 mM NaCl solutions that contained no polymer. Polymer layers were allowed to adsorb for 2 h, before rinsing with 0.1 mM NaCl solutions to make streaming current measurements.

2.8 CE separation conditions and data analysis

All dsDNA separations were carried out using a BioRad BioFocus 3000 (Hercules, CA) in fused-silica capillaries having an ID of 50 μm and a total length of 44.5 cm (39.5 cm effective). The pBR322-*Msp*I digest dsDNA (1 mg/mL in 10 mM Tris-HCl and 1.0 mM EDTA) was diluted 1:10 in 18 MΩ water and dialyzed against water for 10 min using a floating 0.025 μm pore size filter (Millipore). Separation matrix, 3.0 w/v % 1.2 MDa LPA, was dissolved in 1 × TTE (50 mM Tris, 50 mM TAPS, 2 mM EDTA). Prerun electrophoresis was performed at 169 V/cm for 5 min; sample injection was electrokinetic (337 V/cm, 3 s). Separations were performed at 169 V/cm. The current for each run was approximately 3.4 μA. Raw dsDNA separation data were fitted into Gaussian peaks using PeakFit™ 4.06 (SPSS, Chicago, IL, USA); analyte migration times and full temporal width of the peak at half-maximum (FWHM) were then estimated for each peak. Separation efficiency was calculated according to [36]:

$$N = \frac{t^2}{\sigma^2} = \frac{t^2}{(\mathrm{FWHM}/2.35)^2} \quad (2)$$

where *N* is the separation efficiency (number/m), *t* is the peak migration time in seconds, and σ is the peak variance in seconds.

3 Results and discussion

3.1 EOF suppression

The structures of the monomers used in this study, including acrylamide, DMA and DEA, are shown in Table 1. The chemical structures of the monomers dictate that acrylamide is more hydrophilic than DMA [37], which in turn is more hydrophilic than DEA. Table 2 lists the compositions of the DEA/DMA copolymers used in this study. ^{1}H NMR analysis shows that DEA content in the DEA/DMA copolymers is close to the original comonomer composition, which indicates that the reactivity of the comonomers were very similar under our reaction conditions [27]. Hence, random copolymers were formed. Physical characteristics for all polymers studied, including weight-average molar mass (M_w), weight-average radius of gyration (R_g), polydispersity index (PDI), number average degree of polymerization (X_n), and refractive index increment (d*n*/d*c*) are listed in Table 3.

Although it is important to understand the adsorption behavior of dynamic polymeric coatings, critical practical requirements for the success of DEA/DMA copolymers as wall coatings for CE include effective suppression of EOF and adequate separation efficiency for a desired separation technique. We have investigated the electroosmotic mobility within fused-silica capillaries immediately after capillary pretreatment with low concentrations of a weak base, which serves to remove contaminants from the microchannel surface [38], and immediately after flushing with low-viscosity aqueous solutions of the polymer of interest. The electroosmotic mobility within capillaries after pretreatment and immediate following coating with

Table 1. Chemical structures of acrylamide, DMA, and DEA

Monomer	Chemical structure
Acrylamide	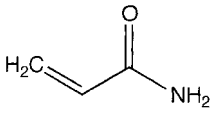
DMA	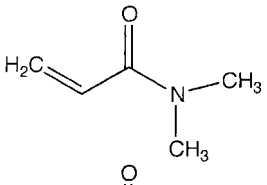
DEA	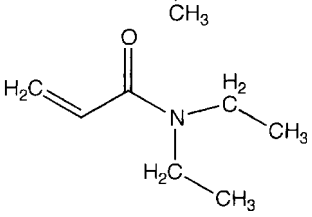

Table 2. Comparison of the monomer ratio (by mass) in the copolymer feed solutions and that in the synthesized copolymers

Polymer	DMA:DEA in feed	DMA:DEA in copolymer
PDEA10	90:10	89:11
PDEA30	70:30	70:30
PDEA50	50:50	50:50
PDEA70	30:70	28:72

DEA/DMA copolymers having similar contour lengths is shown in Fig. 1. Uncoated capillaries after base treatment followed by a water rinse have a high electroosmotic mobility. The results shown in Fig. 1 indicate that PDMA, PDEA10, and PDEA30 provide sufficient EOF suppression for most DNA separation applications. As the hydrophobicity of the dynamic coating polymer increases, the electroosmotic mobility within the coated capillary also systematically increases. This general result indicates that more hydrophobic DEA/DMA copolymers are less able to suppress EOF because their adsorbed hydrodynamic layer thicknesses are too small relative to the thickness of the electrical double layer. The capillary-to-capillary reproducibility of EOF suppression using the same dynamic coating polymer was excellent (data not shown), with a less than 5% failure rate. LPA does not significantly suppress EOF, providing only a minor reduction in electroosmotic mobility within the capillary.

Polymer chemical and physical properties should affect adsorption behavior because of both polymer-solvent and polymer-surface interactions. Although the silica

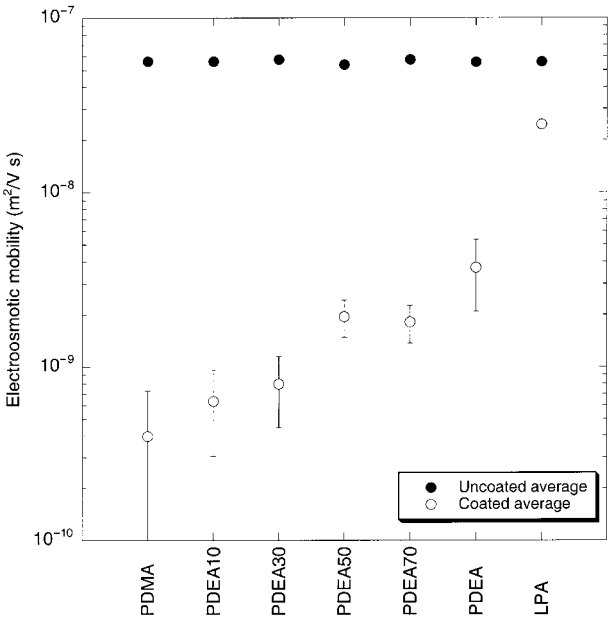

Figure 1. Electroosmotic mobility in fused-silica capillaries (●) immediately following pretreatment with base and (○) immediately following adsorptive coating for different polymer chemistries with similar contour lengths. Error bars denote the standard deviation of the electroosmotic mobility measurements (n = 3 for uncoated capillaries, n = 5 or 6 for coated capillaries).

adsorption behavior of a variety of homopolymers and block copolymers has been investigated in depth [39–42], the silica adsorption behavior of random, neutral copolymers is significantly less well understood. In a theoretical study of random copolymers consisting of segments having two energetically different states, van Lent *et al.* [43] modeled the adsorption behavior of monodisperse random copolymers having a statistical distribution of polymer sequences. Unlike the melt-brush adsorption conformation normally predicted for diblock copolymers in which one block preferentially adsorbs to the surface, random copolymer chains appear to adsorb in a conformation similar to that expected for an adsorbing homopolymer. Amiel *et al.* [44] experimentally investigated the silica adsorption behavior of polydisperse, random poly(*N,N*-dimethylacrylamide-*co*-glycidyl acrylate) from chloroform, which is a good solvent for both monomers. It was postulated that both the DMA and glycidyl acrylate monomers interact with the silica surface *via* carbonyl-silanol hydrogen bonding, but that DMA interacts more strongly due to entropic effects.

Although carbonyl-silanol hydrogen bonding is one important polymer-surface interaction that can occur [45, 46], for our DEA/DMA copolymers the solvent qualities of water for PDEA and PDMA are significantly differ-

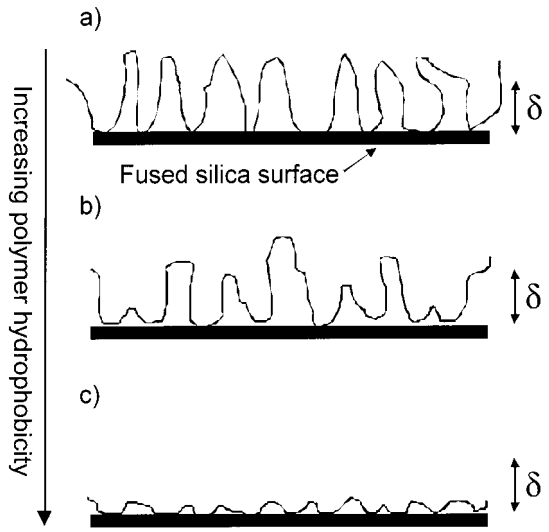

Figure 2. Schematic of possible adsorbed polymer conformations. (a) Polymer with minimal hydrophobic character assumes an adsorbed conformation based both on sterics and on favorable polymer/solvent interactions. (b) Moderately hydrophobic copolymers adsorb in a less "loopy" conformation based on the placement of the "hydrophobic" segments. (c) As the molar percentage of "hydrophobic" segments in the copolymer increases, the polymer adsorbs in a flatter conformation that is less likely to shift the hydrodynamic plane of shear beyond the electrical double layer δ.

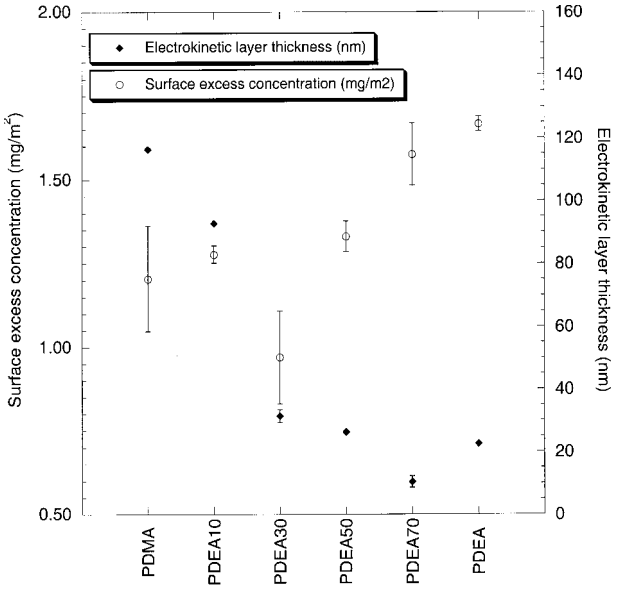

Figure 3. (○) Surface excess concentration and (◆) electrokinetic layer thickness as a function of DEA percent (by mass) of dynamically adsorbed polymer or copolymer. Error bars denote the standard deviation of the surface excess concentration or the electrokinetic layer thickness measurement.

ent, so that polymer adsorption behavior should not be controlled by hydrogen bonding affinities alone. In particular, the ethyl groups of the more hydrophobic monomer DEA should also interact with the silica surface in order to release structured water molecules in an entropically favorable manner [47]. Although carbonyl hydrogen bonding and hydrophobic interactions are likely occurring, there should be a systematic relationship between DEA/DMA copolymer hydrophobicity and adsorbed polymer conformation. A schematic of proposed polymer adsorption behavior is shown in Fig. 2.

We hypothesized that if a "hydrophilic" homopolymer has the potential to adsorb to the silica surface, the polymer should assume an adsorbed conformation based both on sterics and on favorable solvent/polymer interactions, which may result in a polymer layer thickness larger than the electrical double layer thickness δ. If the adsorptive monomer is randomly copolymerized with a more "hydrophobic" monomer, it will have a conformation that is based on the placement of the "hydrophobic" segments near the surface, where they can be sequestered from solvent. As the molar percentage of "hydrophobic" segments is increased, the polymer should assume a flatter conformation in order to release ordered water molecules. To test this hypothesis, the surface concentration and thickness of the adsorbed polymer layer were investigated *via* scanning angle reflectometry and streaming current measurements.

3.2 Conformation of the adsorbed layer

Surface excess concentrations and electrokinetic layer thicknesses determined for PDEA, PDMA, and DEA/DMA copolymers are shown in Fig. 3. The surface excess concentration for LPA was also determined, but the layer thickness could not be determined due to gelation in the streaming current flow cell and hence is not shown. The data shown in Fig. 3 correspond to adsorption plateaus. Except for LPA, adsorption kinetics for the different polymers were very similar, reaching an adsorption plateau in well under one hour. The fastest adsorption kinetics were exhibited by PDEA10 and PDEA30, which required only 5 and 9 min to reach 95% of the plateau (τ_{95}), respectively. For PDMA and PDEA, the times required to reach 95% of the plateau were 19 ± 9 min and 26 ± 2 min, respectively. PDEA50 adsorbed the most slowly, with a τ_{95} of 48 ± 2 min.

The times required to reach the adsorption plateau are determined by the dynamics of polymer configurational relaxations in the adsorbed layers. These dynamics depend on the copolymer composition in a nonmonotonic fashion, with PDEA50 layers requiring significantly longer times to fully develop. Since the standard protocol for preparing dynamic coatings for the EOF suppression experi-

ments allows polymers to adsorb for only 20 min, it is likely that the PDEA50 layer had not fully developed. This may explain why the suppression of EOF by PDEA50, shown in Fig. 1, appears to be slightly less effective than the trend data for the other copolymers would indicate.

LPA adsorption was biphasic, reaching a transient plateau containing approximately 0.12 mg/m^2 after the first 2 h. When continuing the experiment without interruption, a second adsorption regime followed and produced a layer containing 2.3 $\pm$ 0.16 mg/m^2. This second regime reached 95% of its adsorption plateau in 18 $\pm$ 5 h. This unusual adsorption behavior may be attributed to LPA gelation *via* inter- and intrachain hydrogen bonding. All of the polymers were strongly adsorbed, showing less than 10% desorption upon rinsing with polymer-free solutions for as long as 2 h. Typically, 60–70% of the layer remained adsorbed even after 15–18 h of rinsing. The PDEA30 copolymer displayed the least desorption. While LPA provided the maximum adsorbed amount, this was a gelation phenomenon; no evidence of gelation for any of the other polymers was observed. With regard to the effectiveness of the adsorbed polymer layer in the suppression of EOF, the electrokinetic layer thickness is far more revealing than the surface excess concentration.

Polymers of modest hydrophobicity, including PDMA and PDEA10, produced significantly thicker adsorbed layers than the more hydrophobic DEA/DMA copolymers or PDEA. PDMA and PDEA10 layers were 93 and 116 nm thick, sufficient to nearly eliminate the zeta potential (and thereby nearly eliminate all electrokinetic effects). The PDMA and PDEA10 adsorbed layers reduced the zeta potential to –2 to –4 mV (from a bare surface zeta potential of –113 $\pm$ 14 mV). The standard deviation in zeta potentials indicates surface-to-surface variability. Individual measurements are precise to within approximately 1 mV. As the results in Fig. 3 indicate, ζ_{ads} was significant for the more hydrophobic DEA/DMA copolymers, with PDEA70 displaying the smallest reduction in zeta potential. It is interesting to note that the adsorbed layers produced by the more hydrophobic polymers, including PDEA70 and PDEA, have the largest surface excess concentration and the thinnest layers, *i.e.*, they are the most dense. Although increasing polymer hydrophobicity enhances adsorption, a dense (less "loopy") conformation of the adsorbed polymers results from this by solvophobicity and diminishes their ability to suppress EOF, as shown schematically in Fig. 2.

3.3 Impact of polymer contour length

In addition, the contour length of the dynamic coating polymer affects adsorption behavior, which should directly impact EOF suppression capabilities. To study this, the electroosmotic mobilities within capillaries dynamically coated with PDMA or PDEA30 of various contour lengths is shown in Fig. 4. Again, uncoated capillaries treated with dilute solutions of a weak base exhibit a high electroosmotic mobility. As the contour length of PDMA or PDEA30 increases, the electroosmotic mobility within the coated capillary decreases dramatically. PDMA and PDEA30 comprising fewer than 5000 monomer units reduce the electroosmotic mobility within the capillaries by one order of magnitude; a much more significant drop in electroosmotic mobility is observed if the adsorptive coating polymer contains more than 15 000 monomer units. For practical purposes, an electroosmotic mobility of 10^{-9} m^2/Vs or less is adequate for most dsDNA and ssDNA sequencing applications.

As the average contour length of an adsorptive polymer increases, it can be expected that the adsorbed layer formed by these polymers is less mobile [48] and undergoes slower exchange with nonadsorbed chains or chain parts [49] due to an increasing number of polymer-surface contacts. In addition, hydrodynamic layer thickness has been shown to be directly dependent on molar mass, when the former is measured by photon correlation spectroscopy (PCS) [50] and electrokinetic sonic amplitude (ESA) [51]. Competitive adsorption within a relatively polydisperse sample has been shown to occur over relatively long time scales [52, 53], so the effects of the competitive displacement of average contour length chains by higher-molar-mass chains during our microchannel wall coating step should be minimal.

3.4 DNA separation performance

The effect of wall coating hydrophobicity on DNA separation performance was examined using PDMA, PDEA, and DEA/DMA copolymers matched for contour length as dynamic microchannel wall coatings, and a low-molar-mass LPA as the sieving matrix for pBR322-*Msp*I digest DNA. It should be noted that, unlike other studies of dynamic microchannel wall coatings [9, 21, 54, 55], our dynamic coating polymer was not included in the sieving matrix and the surface was not reconditioned or recoated between runs.

Typical dsDNA separations using low-molar-mass LPA (denoted "LPA-matrix" in Table 3) as the separation matrix are shown in Fig. 5. Using low-molar-mass LPA and a variety of dynamic coating polymers, dsDNA fragments ranging from 67 to 622 bp are baseline-resolved, with some resolution of the 147 bp fragment pair. The pairs of 34 bp and 26 bp fragments each appear as a single peak. Qualitatively, it can be observed that while all adsorptive coatings we tested (PDMA, PDEA10, PDEA30, PDEA50,

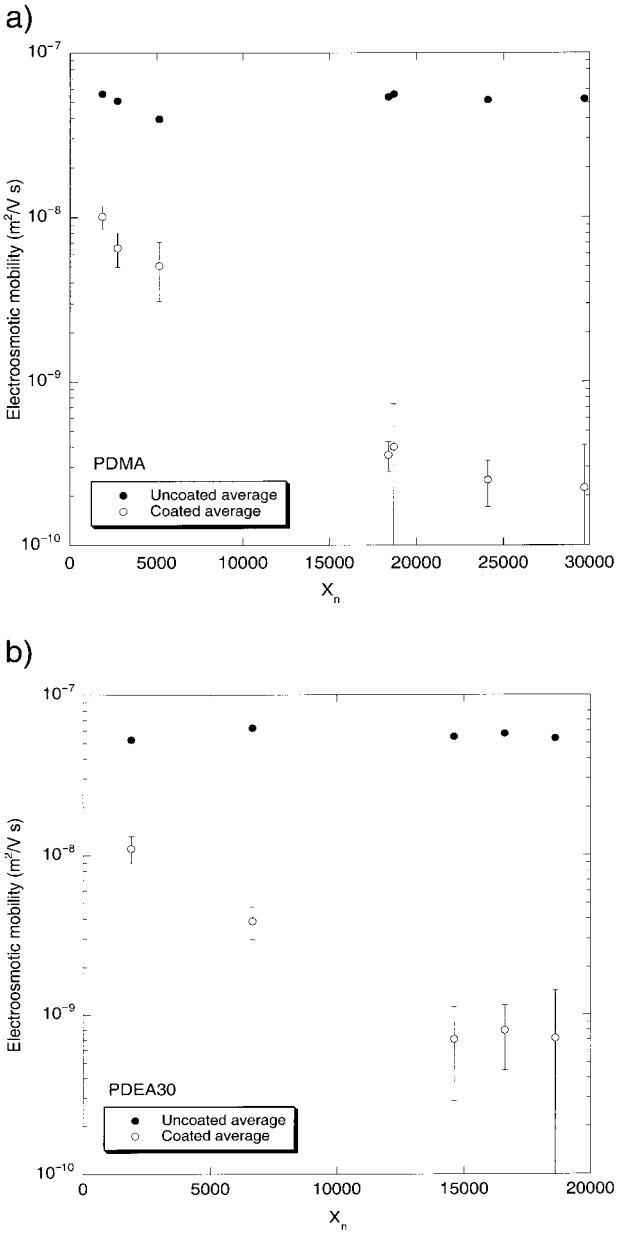

Figure 4. (a) Electroosmotic mobility in fused-silica capillaries (●) immediately following pretreatment with base and (○) immediately following adsorptive coating for PDMAs of different contour lengths. (b) Electroosmotic mobility in fused-silica capillaries (●) immediately following pretreatment with base and (○) immediately following adsorptive coating for PDEA30s of different contour lengths. Error bars denote the standard deviation of the electroosmotic mobility measurements (n = 3 for uncoated capillaries, n = 5 or 6 for coated capillaries).

PDEA70, PDEA) allow good separations, the dsDNA fragment migration times increase monotonically as the hydrophobicity of the dynamic coating polymers, which have been matched for contour length, increases. To illus-

Table 3. Polymer physical characteristics

Matched contour length polymers					
Name	M_r (MDa)	PDI	X_n ($\times 10^{-4}$)	R_g (nm)	dn/dc (mL/g)
LPA	3.60	1.58	2.00	132	0.181
PDMA	2.60	1.40	1.87	112	0.167
PDEA10	3.50	1.94	1.77	142	0.170
PDEA30	3.60	2.02	1.66	114	0.156
PDEA50	3.70	1.73	1.89	95	0.163
PDEA70	3.90	1.56	2.11	89	0.153
PDEA	3.70	1.64	1.77	64	0.177
		PDMA			
PDMA-1	0.34	1.82	0.19	75	
PDMA-2	0.57	2.13	0.27	81	
PDMA-3	0.90	2.09	0.52	78	
PDMA-4	3.80	2.08	1.84	132	
PDMA-5	2.60	1.40	1.87	112	
PDMA-6	4.50	1.88	2.41	146	
PDMA-7	4.57	1.55	2.97	138	
		PDEA30			
PDEA30-1	0.34	1.67	0.19	51	
PDEA30-2	0.76	1.31	0.67	60	
PDEA30-3	3.60	2.29	1.46	126	
PDEA30-4	3.60	2.02	1.66	114	
PDEA30-5	4.00	2.00	1.86	127	
		LPA sieving matrix			
LPA-matrix	1.27	2.27	0.79	88	

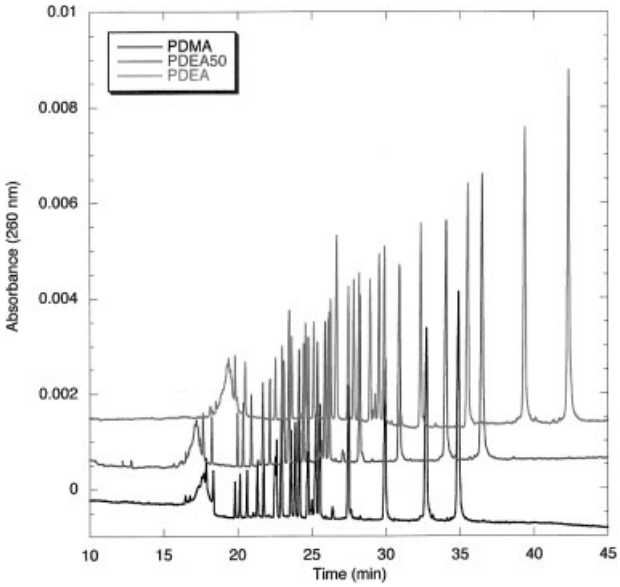

Figure 5. Typical dsDNA electropherograms, using LPA as the sieving matrix, in fused-silica capillaries dynamically coated with PDMA (black line), PDEA50 (blue line), and PDEA (red line) of similar contour lengths. Electrophoresis conditions and capillary coating procedures are described in Section 2.8.

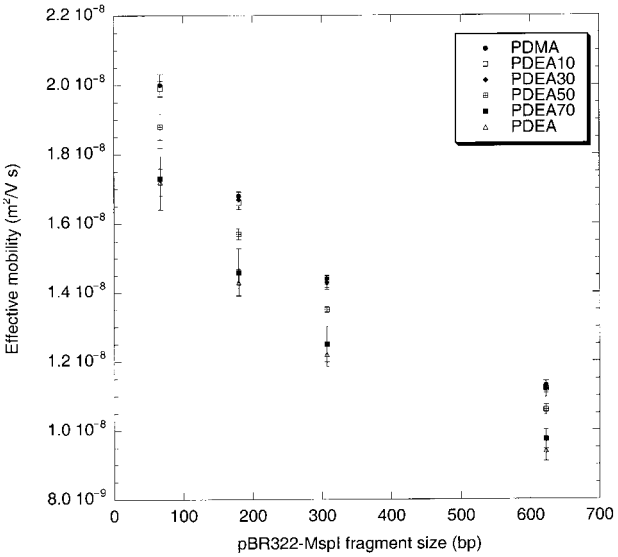

Figure 6. Effective mobilities of selected dsDNA fragments of pBR322-*Msp*I for different dynamic coatings. Electrophoresis conditions and capillary coating procedure are given in Section 2.8. Error bars indicate the standard deviation of the effective mobility (n = 5).

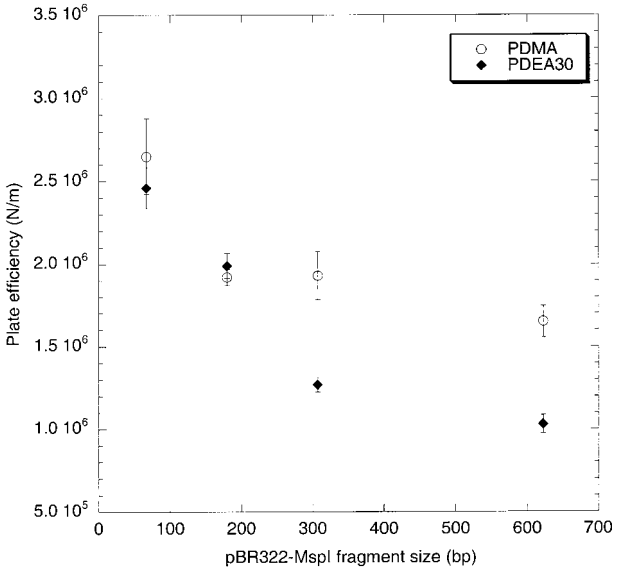

Figure 7. Effect of coating polymer hydrophobicity on pBR322-*Msp*I separation. Wall coatings were matched for their electroosmotic mobility. Error bars denote the standard deviation (n = 3). Conditions: see Section 2.8.

trate this effect, the effective mobilities of the 67, 180, 307, and 622 bp fragments of pBR322-*Msp*I are plotted in Fig. 6 for PDMA, PDEA50 and PDEA.

For all of the fragment sizes analyzed, the effective dsDNA mobility is found to decrease with increasing hydrophobicity of the dynamic wall coating polymer. In particular, it is interesting to note that separations within capillaries dynamically coated with PDMA, PDEA10, or PDEA30 have comparable mobilities, but separations within capillaries dynamically coated with more hydrophobic copolymers or PDEA show significantly diminished effective mobilities. Since, for dynamic coating polymers that have been matched for contour length, polymer hydrophobicity and EOF suppression performance are directly related, it is unclear whether the dsDNA fragment mobility is affected by analyte-wall interactions as well as by residual EOF within the capillary. In order to determine the contribution of analyte-wall interactions, the dsDNA separation efficiency provided by two dynamically coated capillaries that demonstrate equivalent EOF suppression, yet have different polymer chemistries, was ascertained.

The dsDNA separation efficiencies within capillaries dynamically coated with PDMA-2 or PDEA30 are compared in Fig. 7. Again, all separations were performed in "LPA-matrix". There is a minimal difference in the EOF suppression capabilities of PDMA-2 and PDEA30, but there is a pronounced difference in the dsDNA separation performance (plate efficiency) within the two capillaries. Separations within the capillaries dynamically coated with PDEA30 or PDMA-2 were nearly equivalent for dsDNA fragment sizes of less than approximately 200 bp, but the separation efficiencies of larger fragments are markedly different. The lower efficiency of separations of long dsDNA fragments within the capillary dynamically coated with PDEA30 is indicative of increased analyte-wall interactions, since larger DNA is expected to be more hydrophobic. Hence, this small increase in dynamic coating polymer hydrophobicity has a significant effect on DNA separation performance. Analyte interactions with hydrophobic wall coatings, even if the wall coating was able to effectively suppress EOF, could be expected to be much more deleterious in the case of ssDNA or protein analytes, which are substantially more prone to surface adsorption on glass than dsDNA.

4 Concluding remarks

Although adequate dynamic wall coatings exist for some types of DNA separations, it will be important to determine the general requirements for effective wall coatings as well as applicability for other biomolecule analyses, including single-stranded conformational polymorphism/heteroduplex analysis (SSCP/HA) and a wide variety of protein separation techniques, so that the advantages of dynamic microchannel coatings may be extended to these techniques. We find that neutral acrylamide-based polymers employed as adsorptive wall coatings should

contain more than 15 000 monomer units, and should be as hydrophilic as possible in order to adsorb in a "loopy" conformation that shifts the hydrodynamic plane of shear beyond the electrical double layer. However, in the case of these acrylamides, our observations indicate they should also be somewhat hydrophobic in order to adsorb effectively to the microchannel wall (*i.e.,* PDMA *vs.* LPA). Other mechanisms of stabilizing adsorbed polymer layers might also be possible. Finally, the separation efficiency of differently sized dsDNA fragments within dynamically coated capillaries that provide similar EOF suppression, yet possess different hydrophobicities, indicates that the solvophobicity of the microchannel wall coating polymer must be minimal in order to lessen analyte-wall interactions. Minimizing the hydrophobicity of the microchannel wall coating will be particularly crucial for ssDNA or protein analysis. Ongoing work in our laboratory has shown that the PDMA, PDEA, and DEA/DMA copolymers employed as dynamic coatings in this work are not suitable for the separation of SSCP/HA products or for proteins. The investigation of other novel, acrylamide-based polymers and copolymers as wall coatings is currently underway in our laboratory.

The authors gratefully acknowledge technical assistance from Dr. Felicia Bogdan at Northwestern University. Financial support and equipment for this work were provided by the National Institutes of Health (Grant R01HG01970-01), and by ACLARA BioSciences, Inc. Acknowledgement is also made to the donors of The Petroleum Research Fund, administered by the ACS, for partial support of this research. Some experimental work for this study was performed in the Keck Biophysics Facility at Northwestern University (www.biochem.northwestern.edu/keck/keckmain.html). The authors also wish to thank Jim Osborne and Steve Pentoney (Beckman-Coulter, Inc.) for the gift of the P/ACE 5000.

Received November 21, 2001

5 References

[1] Freemantle, M., *Chem. Engineer. News* 1999, 27–36.

[2] Chiari, M., Cretich, M., Damin, F., Ceriotti, L., Consonni, R., *Electrophoresis* 2000, *21*, 909–916.

[3] Horvath, J., Dolník, V., *Electrophoresis* 2001, *22*, 644–655.

[4] Barron, A. E., *Sep. Purif. Methods* 1995, *24*, 1–118.

[5] Hjertén, S., *J. Chromatogr.* 1985, *347*, 191–198.

[6] Pagac, E. S., Prieve, D. C., Solomentsev, Y., Tilton, R. D., *Langmuir* 1997, *13*, 2993–3001.

[7] Fleer, G. J., Cohen Stuart, M. A., Scheutjens, J. M. H. M., Cosgrove, T., Vincent, B., *Polymers at Interfaces*, Chapman & Hall, New York 1993.

[8] Chiari, M., Gelain, A., in: Heller, C. (Ed.), *Analysis of Nucleic Acids by Capillary Electrophoresis*, Vieweg Press, Braunschweig 1997, pp. 135–173.

[9] Gilges, M., Kleemis, M. H., Schomburg, G., *Anal. Chem.* 1994, *66*, 2038–2046.

[10] Karger, B. L., Goetzinger, W., *Polyvinyl Alcohol (PVA) Based Covalently Bonded Hydrophilic Coating for Capillary Electrophoresis*, Northeastern University, Boston, MA, USA 1997.

[11] Chiari, M., Nesi, M., Sandoval, J. E., Pesek, J. J., *J. Chromatogr. A* 1995, *717*, 1–13.

[12] Bruin, G. J. M., Chang, J. P., Kuhlman, R. H., Zegers, K. J. C. K., Poppe, H., *J. Chromatogr.* 1989, *471*, 429–436.

[13] Shao, X., Shen, Y., O'Neill, K., Lee, M. L., *Chromatographia* 1999, *49*, 299.

[14] Chiari, M., Dell'Orto, N., Gelain, A., *Anal. Chem.* 1996, *68*, 2731–2736.

[15] Huang, M., Plocek, J., Novotny, M. V., *Electrophoresis* 1995, *16*, 396–401.

[16] Shao, X., Shen, Y., O'Neill, K., Lee, M. L., *J. Chromatogr. A* 1999, *830*, 415–422.

[17] Huang, X., Doneski, L. J., Wirth, M. J., *Anal. Chem.* 1998, *70*, 4023–4029.

[18] Chiari, M., Cretich, M., Stastna, M., Radko, S. P., Chrambach, A., *Electrophoresis* 2001, *22*, 656–659.

[19] Katayama, H., Ishihama, Y., Asakawa, N., *Anal. Sci.* 1998, *14*, 407.

[20] Katayama, H., Ishihama, Y., Asakawa, N., *Anal. Chem.* 1998, *70*, 5272.

[21] Rodriguez, I., Li, S. F. Y., *Anal. Chim. Acta* 1999, *383*, 1–26.

[22] Mathur, S., Mougdil, B. M., *J. Coll. Int. Sci.* 1997, *196*, 92–98.

[23] Madabhushi, R. S., *Electrophoresis* 1998, *19*, 224–230.

[24] Gao, Q. F., Yeung, E. S., *Anal. Chem.* 1998, *70*, 1382–1388.

[25] Chiari, M., Cretich, M., Horvath, J., *Electrophoresis* 2000, *21*, 1521–1526.

[26] Ren, J. C., Fang, Z. F., *Chin. Chem. Lett.* 2000, *11*, 1015–1018.

[27] Song, L., Liang, D., Kielescawa, J., Liang, J., Tjoe, E., Fang, D., Chu, B., *Electrophoresis* 2001, *22*, 729–736.

[28] Cifuentes, A., Diez-Masa, J. C., Fritz, J., Anselmatti, D., Bruno, A. E., *Anal. Chem.* 1998, *70*, 3458–3462.

[29] Albarghouthi, M. N., Buchholz, B. A., Doherty, E. A. S., Bogdan, F. M., Zhou, H., Barron, A. E., *Electrophoresis* 2001, *22*, 737–747.

[30] Williams, B. A., Vigh, G., *Anal. Chem.* 1996, *68*, 1174–1180.

[31] Tilton, R. D., in: Dubin, P., Farinato, R. (Ed.), *Polymer-Colloid Interactions: Techniques and Applications*, John Wiley and Sons, New York 1999, pp. 331–363.

[32] Furst, E. M., Pagac, E. S., Tilton, R. D., *Ind. Eng. Chem. Res.* 1996, *35*, 1566–1574.

[33] Velegol, S. B., Tilton, R. D., *Langmuir* 2001, *17*, 219.

[34] Fu, Z., Santore, M. M., *Colloids and Surfaces A: Physicochemical and Engineering Aspects* 1998, *135*, 63.

[35] Braem, A., *PhD Dissertation,* Carnegie Mellon University, Pittsburgh, PA 2001.

[36] Grossman, P. D., *J. Chromatogr. A* 1994, *663*, 219–227.

[37] Gelfi, C., P., D. B., Alloni, A., Righetti, P. G., *J. Chromatogr.* 1992, *608*, 333–341.

[38] Kaupp, S., Bubert, H., Baur, L., Nelson, G., Wätzig, H., *J. Chromatogr. A* 2000, *894*, 73–77.

[39] Amiel, C., Sikka, M., Schneider, J., James, W., Tsao, Y.-H., Tirrell, M., Mays, J. W., *Macromolecules* 1995, *28*, 3125–3134.

[40] Parnas, R. S., Chaimberg, M., Taepaisitphongse, V., Cohen, Y., *J. Coll. Interface Sci.* 1989, *129*, 441.

[41] Char, K., Gast, A. P., Frank, C. W., *Langmuir* 1988, *4*, 989.

[42] Bijsterbosch, H. D., Cohen Stuart, M. A., Fleer, G. J., *Macromolecules* 1998, *31*, 9281–9294.

[43] van Lent, B., Scheutjens, J. M. H. M., *J. Phys. Chem.* 1990, *94*, 5033–5040.

[44] Amiel, C., Sebille, B., *J. Coll. Interface Sci.* 1992, *149*, 481–492.

[45] Amiel, C., Sebille, B., Hommel, H., Legrand, A. P., *J. Coll. Interface Sci.* 1994, *165*, 236–243.

[46] Yamagiwa, S., Kawaguchi, M., Kato, T., Takahashi, A., *Macromolecules* 1989, *22*, 2199–2203.

[47] Inomata, H., Goto, S., Saito, S., *Macromolecules* 1990, *23*, 4887–4888.

[48] Sukhishvili, S. A., Chen, Y., Müller, J. D., Gratton, E., Schweizer, K. S., Granick, S., *Nature* 2000, *406*, 146–146.

[49] Mubarekyan, E., Santore, M. M., *Macromolecules* 2001, *34*, 4978–4986.

[50] Killmann, E., Maier, H., Kaniut, P., Gutling, N., *Colloids and Surfaces* 1985, *15*, 261–276.

[51] Maier, H., Baker, J. A., Berg, J. C., *J. Coll. Interface Sci* 1987, *119*, 512–517.

[52] Dijt, J. C., Cohen Stuart, M. A., Fleer, G. J., *Macromolecules* 1992, *25*, 5416–5423.

[53] Dijt, J. C., Stuart, M. A. C., Fleer, G. J., *Macromolecules* 1994, *27*, 3219–3228.

[54] Chiari, M., Damin, F., Reijenga, J. C., *J. Chromatogr. A* 1998, *817*, 15–23.

[55] Iki, N., Yeung, E. S., *J. Chromatogr. A* 1996, *731*, 273–282.